COBEM 2023 27TH INTERNATIONAL CONGRESS OF MECHANICAL ENGENEERING

ABCM Brazilian Society of Mechanical Sciences and Engineering
27th ABCM International Congress of Mechanical Engineering
December 04-08, 2023, Florianópolis-SC, Brazil

COB-2023-0611
A NUMERICAL STUDY ON 2D SPATIAL MIXING LAYERS USING SPECTRAL/HP METHODS: INSIGHTS ON HOW MESH REFINEMENT AFFECTS FLOW STATISTICS

Daniel Garcia-Ribeiro
Vinicius Malatesta
Rodrigo C. Moura
Instituto Tecnológico de Aeronáutica - ITA - São José dos Campos, São Paulo, Brazil
danieldgr@ita.br

Abstract. *High-fidelity simulations of turbulent flows have been becoming more feasible in the last years mainly due to the increase of computational power. In this context, the present paper reports results of high-fidelity simulations of a 2D spatial mixing layer. The simulations are achieved by the implicit Large Eddy Simulation (iLES) methodology, or also called as under-resolved Direct Numerical Simulation (uDNS), and the high-order method Continuous Galerkin with the Gradient-Jump penalty stabilization technique are used to simulate the incompressible 2D Navier-Stokes equations and a passive scalar equation. The simulations were started with a hyperbolic tangent profile for the u-velocity and a step profile for the passive scalar. The passive scalar field was resolved in order to observe the mixing between the two fluid layers, which used the same value of the kinematic viscosity as diffusion coefficient (unit Schmidt number). All simulations reported here were run in the open source Nektar++ platform for a Reynolds number, based on the initial momentum thickness, equal to 1000 and provided consistent and expected results for the flow field. These results have been obtained at different levels of mesh refinement and showed an acceptable level of variability due to a slow convergence of flow statistics.*

Keywords: *Mixing layer, scalar mixing, implicit LES, high-order simulation, CFD*

1. INTRODUCTION

Among the many flow types that can be found, the canonical flows are able to represent specific flow phenomena such as flow separation, periodic vortex shedding and boundary layers that are present in many applications. Another example, representing a free shear layer, is the mixing layer, which is when two layers of fluids with different speed slide over each other and provoke a mixture between the fluid. Also, mixing layers have the specific characteristic of a growing Reynolds number (*Re*) with the stream-wise direction, possessing, then, a local feature. The previous condition turns spatial mixing layer an interesting study case because it's possible to observe the evolution of the flow from a laminar to a fully turbulent state, besides others physics phenomena. For specific scaled velocities and coordinates, mixing layers have a constant spreading rate between 0.06 and 0.11, depending on the inlet conditions (Pope, 2000). Therefore, for a Re based on velocity, a characteristic width and fluid's kinematic viscosity, the growth of the Re is linearly in the fully-turbulent region.

There are many studies in the literature that investigated the physics of mixing layers (see e.g. Gaster *et al.* (1985), Koochesfahani and Dimotakis (1986) and Zhang *et al.* (2018)). They have sought to understand how some phenomena occurred and how they were related to others parameters such as Mach number (*Ma*) and inlet conditions. For instance, Stanley and Sarkar (1997) studied the spatial development of a two-dimensional mixing layer using direct numerical simulation (DNS) under different types of inflow forcing with and without background spectrum. They found an increase in the initial growth of the vorticity thickness for the forced inflows, corresponding to a more energized fluctuation field. As the flow develops, the influence on growth rate reduces and negligible differences are found in it when compared to the unforced flow. Others research have also found that same trending of mixing layers' thickness under different inflow conditions (McMullan *et al.*, 2007; Maghrebi and Zarghami, 2010; Martha *et al.*, 2013). As for the *Ma* influences, Foysi and Sarkar (2010) showed that there is a decrease in the mixing layer thickness with the increment of *Ma*, which was in accordance with their experimental reference. Also, they showed that the turbulent intensities are also reduced with the increment of *Ma*, besides that there are an increased spatial decorrelation of turbulence. These compressibility effects had already been encountered by others papers (Papamoschou and Roshko, 1988; Clemens and Mungal, 1992). Reacting mixing layers have also been focus of many studies in order to understand the rate of chemical product formed, their thickness growth and others parameters such as heat release (see e. g. McMurtry *et al.* (1986); Miller *et al.* (1994); Kartha *et al.* (2020)).

To numerically study a mixing layer, common techniques are the DNS or Large Eddy Simulation (LES) approaches

of turbulence, where the last one uses sub-grid models to model the small-scales influence as they are filtered out. The domain size will depend if the study is compared with an wind tunnel test and on the computational power available, but considerations about blockage effects must be in mind in the cross and span wise directions. The stream-wise size will vary upon the necessity to capture the flow structures. In any case, usual lengths are between $25\delta_{\omega,0}$ and $350\delta_{\omega,0}$ or $400\delta_{\theta,0}$ and $1150\delta_{\theta,0}$ in the x-component (stream-wise); $6\delta_{\omega,0}$ and $100\delta_{\omega,0}$ or $290\delta_{\theta,0}$ and $350\delta_{\theta,0}$ in the y-component (cross-wise); $5\delta_{\omega,0}$ and $20\delta_{\omega,0}$ or $10\delta_{\theta,0}$ and $170\delta_{\theta,0}$ in the z-component (span-wise), where $\delta_{\omega,0}$ and $\delta_{\theta,0}$ are the initial vorticity and momentum thickness respectively. The mesh discretization will also vary depending on the turbulence approach and resolution of the LES adopted. As for the initial and boundary conditions, the first one usually follows the inlet condition or set a step-like function between each fluids' velocity, and the boundary conditions are no-slip walls or far-field and outflow for spatial mixing layers or periodicity for time-developing mixing layers (Stanley and Sarkar, 1997; Tenaud *et al.*, 2005; Foysi and Sarkar, 2010; Attili and Bisetti, 2012; Martha *et al.*, 2013; Kartha *et al.*, 2020).

As an alternative to the LES approach, there is the implicit Large Eddy Simulation (iLES), or also called under-resolved Direct Numerical Simulation (uDNS). Instead of using a specific model to simulate the dissipation of the filtered out smallest turbulence scales, the iLES approach relies on the dissipation of the adopted numerical method, such as finite differences, finite volumes and spectral/hp elements (Pope, 2000). This last method may be the Continuous Galerkin (CG) or Discontinuos Galerkin (DG) high-order methods and they apply projections of a set of functions to solve the differential equations of the fluid dynamics. They have been theme of many studies in order to understand their properties and advantages when simulating turbulent flows. For some examples of research studying the CG or DG method, the reader is referred to Moura *et al.* (2017), Moura *et al.* (2019), Ferreira *et al.* (2022) and Martins (2021). In this context, this paper's objective is to simulate a two-dimensional spatial mixing layer with the spectral/hp CG method in order to validate if the method is able to capture the physics identified in others studies. Also, it's sought to define the best simulation set up to enable future three-dimensional simulations, focusing on capturing others flow structure types.

2. MATERIALS AND METHODS

This section describes the numerical methodology adopted in this study, the physical modeling of the mixing layer, the initial and boundary conditions and the mesh study. In sum, all the information necessary to conduct the research.

2.1 Numerical approach

The aforementioned iLES or uDNS methodology is applied herein. Therefore, the solution of the problem counts on the numerical dissipation to model the dissipation of the small length-scales. The high-order spectral/hp element method used is the CG one, which is formulated on Galerkin projections of a given set functions to resolve a defined equation. In our case, the equations solved are the partial differential equations (PDE) hereafter presented.

The 2D mixing layer studied here represents an unsteady incompressible flow free of body-forces and it is composed by a Newtonian fluid. Also, its properties are constant and isotropic. Thus, the fluid dynamics equations reduces to the two-dimensional continuity and momentum equations as follows[1].

$$\nabla \cdot \mathbf{U} = 0 \tag{1}$$

$$\frac{D\mathbf{U}}{Dt} = -\nabla p + \nu \nabla^2 \mathbf{U} \tag{2}$$

where p is the pressure normalized by the fluid density (assumed constant), ρ is the fluid density, μ is the fluid molecular viscosity and $\mathbf{U}$ is the velocity vector. Also $\frac{D}{Dt}$ denotes the so-called material derivative. Besides the above equations, a passive scalar transport equation is solved to observed the mixing between the fluid. This equation is given by:

$$\frac{DQ}{Dt} = D_Q \nabla^2 Q \tag{3}$$

where Q is the passive scalar and D_Q is the constant and uniform scalar diffusivity[1].

Finally, all the simulations were performed in the open-source software Nektar++ with a CG forth-order spatial discretization (P = 3), a spectral/hp dealiasing and GJP stabilization techniques (Moura *et al.*, 2020, 2022). Nektar++ is a software that provides CG and DG methodology and it has been widely used to study turbulence with iLES approach (Cantwell *et al.*, 2015; Moxey *et al.*, 2020; Mengaldo *et al.*, 2021).

2.2 Modeling of the mixing layer and boundary conditions

As presented above, the herein simulated mixing layer is composed by only one incompressible fluid. So, as there are not two fluids with different densities or product formation by a chemical reaction, a passive scalar field is also solved in

[1]Nektar++: Spectral/hp Element Framework - User Guide, Version 5.2.0. Available at: https://www.nektar.info/getting-started/documentation/

order to highlight the mixing occurring among the fluid. Also, the mixing layer is defined by a initial Re based on the kinematic viscosity (ν), the initial momemtum thickness ($\delta_{\theta_0} = 1$) and the velocity difference ($\Delta U = 1$) (see Eq. 4), therefore we assume non-dimensional variables based on the unit thickness and unit velocity difference. Here, the upper and slow free-stream velocity (U_2) is equal to 0.5 and the bottom and fast free-stream velocity (U_1) is equal to 1.5. These velocities yields a velocity difference parameter (λ) equal to 0.5 and a velocity ratio (r) equal to 0.33. See Eq. 5 for their equations.

$$Re_{\delta_{\theta_0}} = \frac{\Delta U\, \theta_0}{\nu} \tag{4}$$

$$\Delta U = U_1 - U_2, \quad \lambda = \frac{U_1 - U_2}{U_1 + U_2} \quad \text{and} \quad r = \frac{U_2}{U_1} \tag{5}$$

The simulation was initialized with $Re_{\delta_{\theta_0}}$ equal to 1000 and the kinematic viscosity is manually adjusted to obtain that ***Re***. The momemtum thickness is given by Eq. 6, where $u(y)$ is the mean stream-wise velocity.

$$\delta_\theta = \int_{-\infty}^{\infty} \frac{u(y) - U_2}{U_1 - U_2} \left(1 - \frac{u(y) - U_2}{U_1 - U_2}\right) dy \tag{6}$$

Another quantity of interest is the convective velocity, which is defined by the average of the velocities ($U_c \equiv \frac{1}{2}(U_1 + U_2)$) and can be interpreted as the mean velocity of a particle travelling trough the domain. Related to this quantity, one can define the flow-through cycle (FTC), which is the time of a particle to leave the domain travelling at the center line velocity (or convective velocity). Finally, as previous described, a mixing layer has a local attribute, so a ***Re*** is defined for each stream-wise location given by the local momemtum thickness.

The domain, as in many other studies, is a quadrilateral with $960\delta_{\theta_0}$ height (y coordinate) and $1000\delta_{\theta_0}$ long (x coordinate). As this is a 2D study, there is no width or z-coordinate. The previous are sizes similar or even bigger than some studies in the literature, so no containment effects are expected. (Stanley and Sarkar, 1997; Tenaud *et al.*, 2005; Foysi and Sarkar, 2010; Attili and Bisetti, 2012; Martha *et al.*, 2013; Kartha *et al.*, 2020). The domain extends -$400\delta_{\theta_0}$ below and $560\delta_{\theta_0}$ above the initial center line because the mixing layer tends upwards as the high-speed fluid is located at the bottom and the respective values were defined after initial simulations in order provide similar distances from the mixing region to the upper and lower surfaces.

A hyperbolic tangent velocity profile was set at the inlet in such a way that it resulted in the defined initial momentum thickness (see Eq. 7). Also at the inlet, the scalar Q values was defined equal to 1 for the high-speed fluid and 0 for the slow-speed one. The upper and lower boundaries were defined as far-field, i.e. Neumann conditions equal to zero for the scalar and velocity components, and Dirichlet condition equal to zero for the pressure. Then, for the outlet, an outflow condition with zero relative pressure was defined. For last, the simulation was started with initial condition for all variables equal to the inlet boundary conditions. Figure 1 shows the aforementioned conditions and lengths.

$$u(y) = U_c - \frac{\Delta U}{2} \tanh\left(\frac{y}{2\delta_{\theta_0}}\right) \tag{7}$$

As said above, the inlet condition is a hyperbolic tangent profile in order to mimic an ideal profile of a mixing layer. It's possible to apply a more realistic inlet profile, as a boundary layer profile, but the studies which have such inlet usually attempts to mimic experimental investigations, which is not the case here. Moreover, there is not any treatment in our simulation to trigger transition to turbulence, although previous attempts showed that introducing velocity fluctuations help to anticipate transition. For the time integration, an implicit-explicit time-stepping second-order scheme (IMEX) was used to march until a physical time t = 40000 with a time-step (*dt*) of 0.01 (equal to a 0.01 non-dimensional time-step $d\tau = dt\frac{\Delta U}{\delta_{\theta 0}}$). The adopted time-step guaranteed a CFL (Courant–Friedrichs–Lewy condition) approximately equal to 0.11 throughout the whole simulation.

2.3 Mesh parameters and study

Towards creating a mesh capable of capturing the flow structures with an acceptable accuracy and having in mind the limited computational cost available, the domain was divided in five surfaces: one for the laminar-transitional part (s1), other for the mixing region (s2), one for transitioning between the laminar-transitional surface to the mixing region surface (s3), and two other for each part (upper and lower) of the domain (s4 and s5). The s1 surface is meshed with structured quadrilateral elements and the elements size follow a geometric progression both in x and y directions. All others surfaces are meshed with unstructured triangular elements. The s3 surface has elements with the same prescribed edge size, whereas the s2 surface was manually adjusted in order to accommodate the change in the mesh between s1 and s2 to not create distorted elements. Surfaces s4 and s5 are the outer regions of the mixing layer and the elements grow in size until the boundaries.

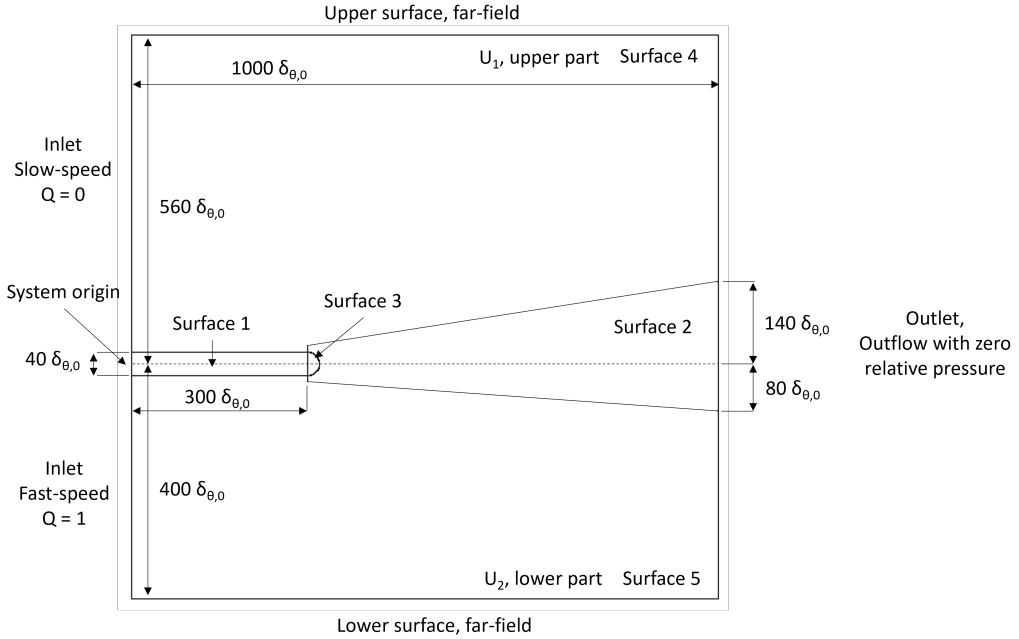

Figure 1: Definition of the domain's features

In the structured region, the geometric progression for the x-direction was defined by the first element length ($dx = 10$), the last one length ($dx = 1$) and the length of the structured region ($l_{struct} = 300$). For the y-direction, the first four elements away from the center line have the same length ($dy = 0.75$). Then, from the fifth element, there are 10 elements that grow with a geometric progression of 1.1. The entire surface s1 has a length of 300 and a height of 40. Figure 1 presents the surfaces delimited in the domain as some lengths and Fig. 2 shows a detail of the mesh in the structured region. Surface s3 is a semi-circumference with radios equal to 20 where the element size was adjusted to smooth the transition between surface 1 and 2, and it has 60 elements in its arc. This last region is also shown in Fig. 2. As going to be explained below, three sizes were applied to surface s3 and the selected one is equal to 2. The heights of the right side of the cone (see Fig 1) were defined after previous simulations in order to contain the whole mixing region throughout the simulation. Figure 2 shows the mesh in this region with the selected edge size. For last, surfaces s4 and s5 have bigger elements to save computational cost as these regions are out of the mixing region.

Besides the geometry manipulation described above, a mesh study was performed in order to check the solution sensitivity to the mesh elements size, specifically inside the mixing region. Some attempts were performed with the structured region, but the modifications resulted in no observable changes. Also, we must have in mind the computational power available and that we are using an iLES strategy, so we do not want to refine the mesh until a DNS approach. Therefore, only the surface s3 had its parameter changed, being them: $l_e = 5$, $l_e = 3$ and $l_e = 2$ for mesh 1, mesh 2 and mesh 3 respectively.

3. RESULTS AND DISCUSSION

In this section, we present the numerical results obtained from the mesh study and physical quantities of interest for the selected mesh in order to defined a suitable numerical setup to run others simulations with specific goals.

3.1 Transient analysis

Although it's known in the literature that unsteady simulations have an initial transient part due to boundary and initial conditions, there are many studies that do not explicitly state how the transient was identified and considered, leaving opened its treatment thus. On the other hand, some studies consider a specific amount of time, might it be based on a physical feature or not, as enough to the transient part of the flow to be finished. In the present flow type, the transient part is defined by the first vortices of the flow. Among those last research, Tenaud *et al.* (2005) stated that the transient had already vanished from the domain after 234 non-dimensional times - based on the velocity difference and initial vorticity thickness. Martha *et al.* (2013) considered that 4 FTCs were enough to the transient end and Kartha *et al.* (2020) considered one convective time - based on the domain length and the lower fluid speed.

Towards identifying the transient and defining a sufficient simulation time to it be finished, we observed the formation of the first eddies in the scalar field, tracked them until they have left the domain to have a first idea of the transient part. Then, we plotted the instantaneous values of the x-velocity component (u), fluctuation kinetic energy ($k = u'^2 + v'^2$) and

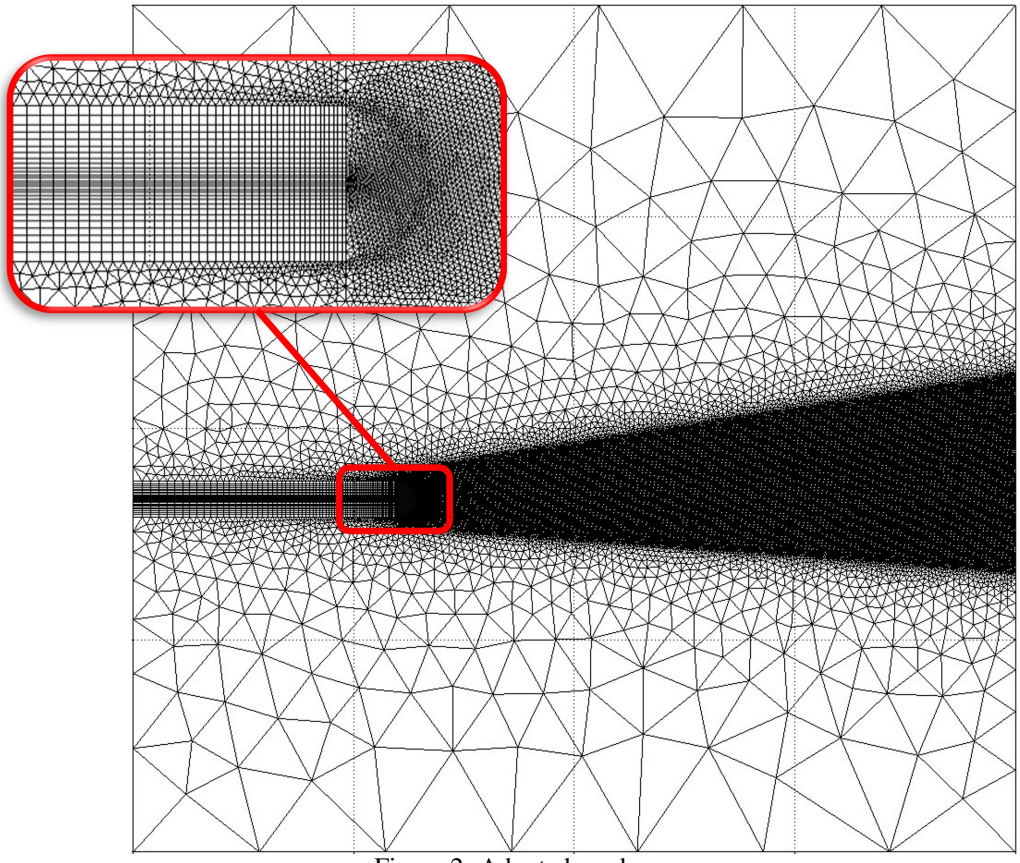

Figure 2: Adopted mesh

pressure (p) to define a big enough time to the end of the transient. These last two procedures were performed for the three studied meshes and the quantities were plotted at (x,y) = (800,0) to lie in the mixing region and far enough from the inlet to capture the real end of the transient. We recall that the structured region is the same for all meshes, so they had the first eddies developing at $x \approx 230$ and $t \approx 300$ and they had completely left the domain at $t \approx 1400$ as it is shown in Fig. 3. This figure also shows the development of the mixing layer, since the rolling-up of the initial Kelvin-Helmholtz vortices until merging and pairing of the vortices, and growth of the layer. One can also notice the increase in the mixed region along the mixing layer.

The instantaneous values and the convergence study (this last one is presented in the next section) were all collected with an output time frequency of 50, i.e. the values were written with a time spacing of $t = 0.5$, and a spatial sampling of 0.2 from $y = -200$ to $y = 200$, which resulted into 2001 data points for each time step. The previous time and spatial sampling were defined after some initial simulations in order to obtain a treatable data file size and to not jeopardize the quality of the results.

Figure 4 presents those instantaneous values until $t = 12000$. Also, a moving average with a time window of $\Delta t = 1000$ (equivalent to a 1 FTC) is shown for each variable. One can see that the greatest discrepancies are found in the initial part until around $t = 1500$, agreeing with some extent with the visual observations of Fig. 3. For the sake of warranty, we considered that the transient and any of its residual effects had already left the domain at a time of 4000. This considered time is equivalent to 4 FTCs or 4000 non-dimensional times based on the convective velocity and the initial momentum thickness, which is a high enough value according to the literature. As a note, the value of the time window was chosen due to its relation with the convective speed and streamwise length, i.e. the mean time necessary for a particle to leave the domain. A lower time window value would approach the curve to the instantaneous values, whereas a higher one would soft the curve, delaying the apparent end of the transient thus.

3.2 Convergence analysis and mesh study

The statistically convergence of the flow is usually obtained by observing time-averaged quantities of interest for enough time. As it happens with the transient analysis, some studies do not show how the convergence was reached and others present it based on different time references. In 3D simulations, Tenaud *et al.* (2005) observed the evolution of vorticity thickness, velocity components and a Reynolds stress tensor component, and concluded that 61.7 non-dimensional times were enough for convergence. On the hand, Attili and Bisetti (2012) calculated the statistics for 3500

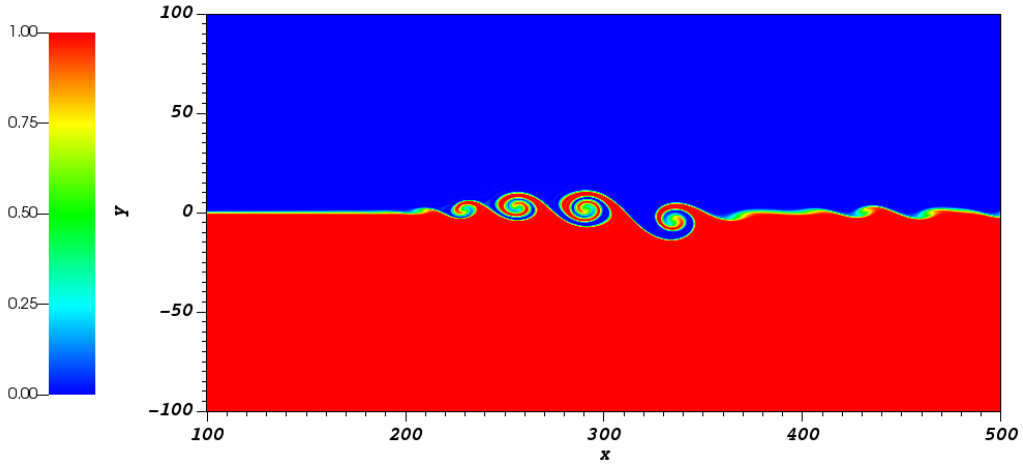

(a) Close look at the first eddies. t = 300

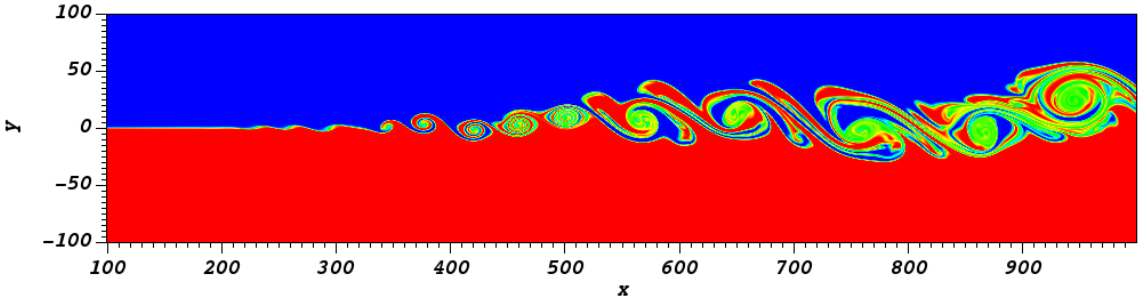

(b) Whole mixing layer after the passage of the firt eddies. t = 1400

Figure 3: Scalar field snapshots of the first eddies formation and when they had completely left the domain

non-dimensional times, which was also based on the velocity difference and the initial vorticity thickness as in Tenaud *et al.* (2005). Martha *et al.* (2013) stated that 8 FTCs were enough for the time-averaged results and Kartha *et al.* (2020) used only four eddy turn-over times - which are based on the largest eddy size and the convective velocity. For 2D simulations, Yang *et al.* (2004) averaged the results during 100 physical times and the others references did not present the time-window used.

Besides studying the statistical convergence, we analysed three different meshes in order to check how the results were changing as explained in Section 2.3. Table 1 presents the mesh parameters of the three studied cases (element sizes of the surface s2, number of elements in the mesh, N_{el}, and number of degrees of freedom, N_{dof}). The N_{dof} was estimated as $N_{el}P^2$ for quadrilateral elements and $\frac{1}{2}N_{el}P^2$ for triangular elements, remembering that P is the order of the polynomial basis. As it can be seen, a reduction in the element size by a factor of 0.4 lead to an increase in element numbers by a factor of 4.08 from Mesh 1 to Mesh 3, showing the disproportional increase of cost when refining the meshes.

Figure 5 shows the evolution of the mixing layer's momentum thickness for each mesh at x = 800. Each data point in the curves represents the accumulated time-averaged results after the transient end, i.e. the data is averaged starting from t = 4000 until that time point. As it can be seen, each mesh tends to converge to a value after a high enough simulation time and we stopped at t = 40000 for considering the simulations reached converged state. The time-window of this average is 36000 physical times, which corresponds to 36 FTC or 36000 non-dimensional times and it falls above the values usually used in the literature, perhaps because this is a 2D simulation (Tenaud *et al.*, 2005; Attili and Bisetti, 2012; Martha *et al.*, 2013; Kartha *et al.*, 2020; Yang *et al.*, 2004). Also, the momentum thickness drops consistently from 10.45 for Mesh 1 to 10.07 for Mesh 3, showing a convergence and an agreement between meshes when one have in mind the differences in degrees of freedom. For the sake of brevity, only the momentum thickness is shown for the mesh study, but we also

Table 1: Meshes' parameters

	Mesh 1	Mesh 2	Mesh 3
l_e	5	3	2
N_{el}	16736	34781	68311
N_{dof}	84888	166091	316976

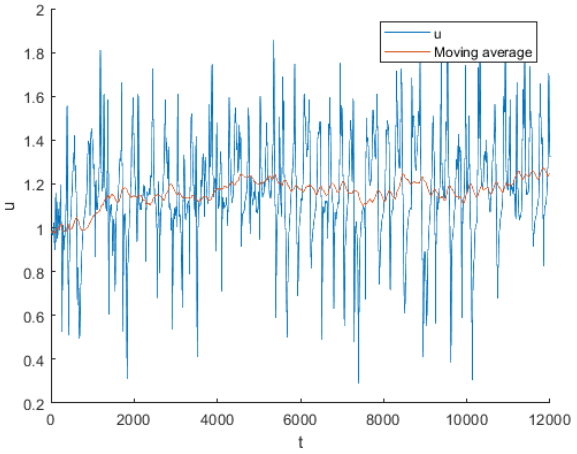

(a) x-velocity component.

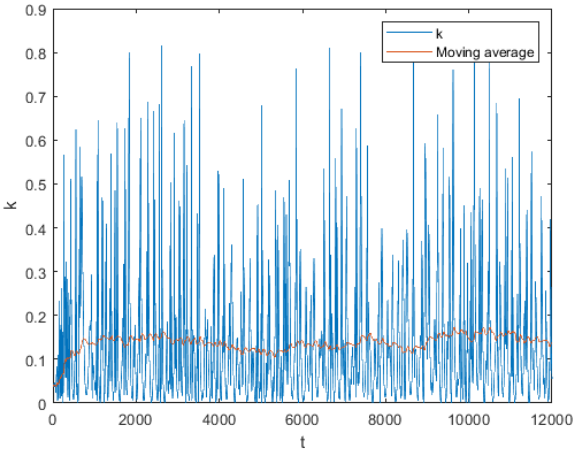

(b) Fluctuation kinetic energy.

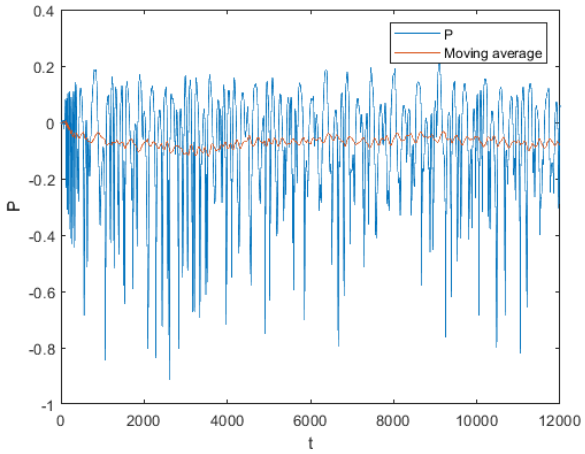

(c) Pressure.

Figure 4: Instantaneous values of velocity components and pressure at (x,y) = (800,0). Moving average with a time window of $\Delta t = 1000$

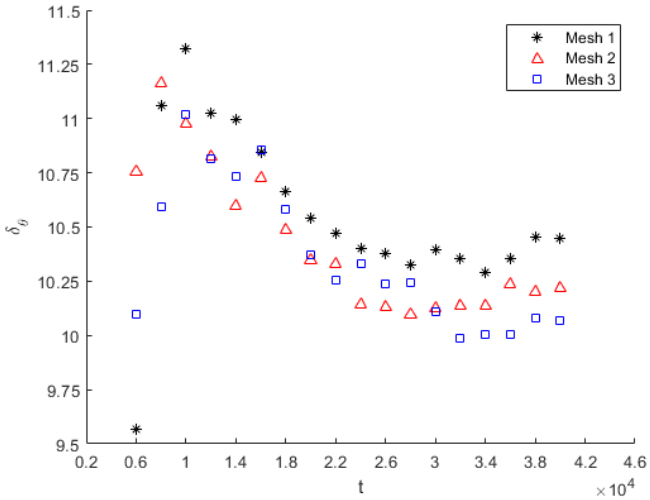

Figure 5: Evolution of the accumulated time-averaged mixing layer's momentum thickness. Time-averaging starts from t = 4000.

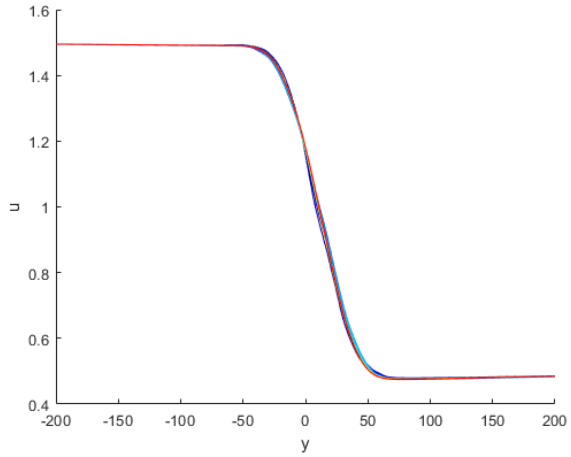

(a) x-velocity component.

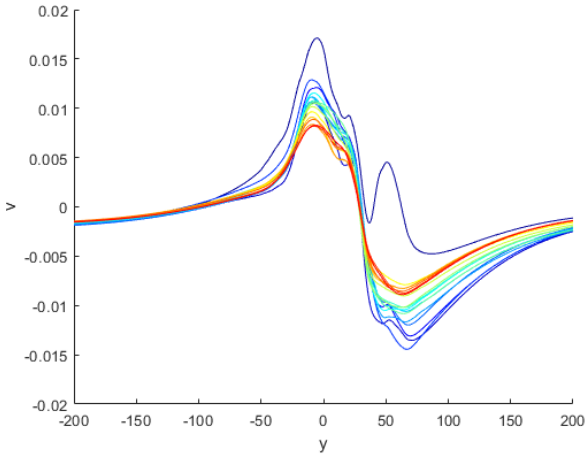

(b) y-velocity component.

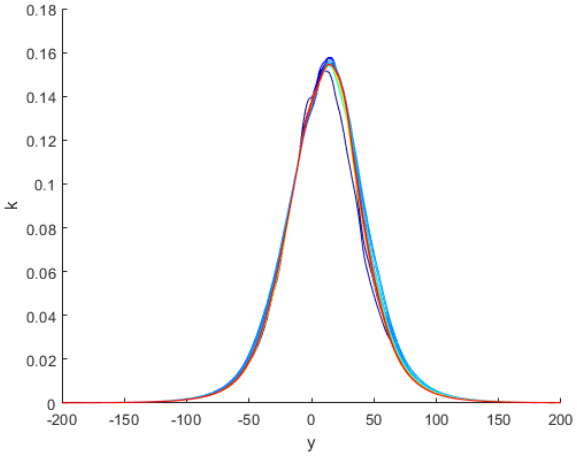

(c) Fluctuation kinetic energy

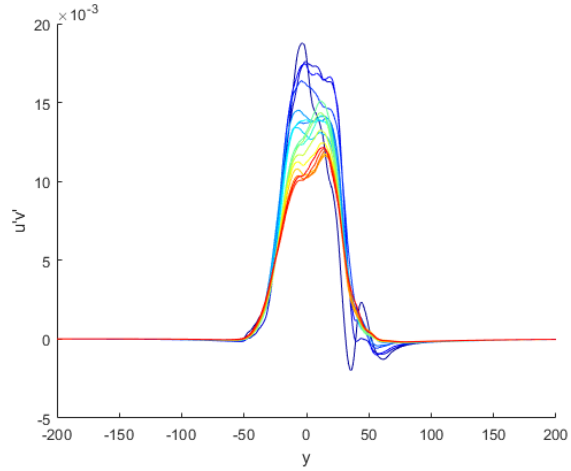

(d) Reynolds stress tensor component

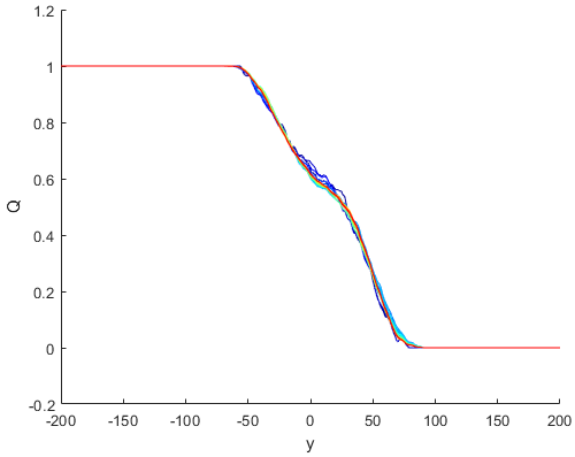

(e) Scalar

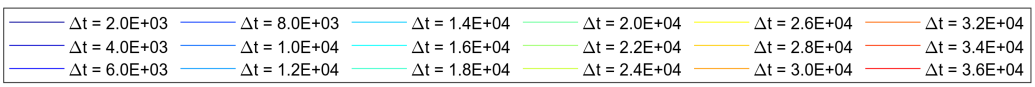

Figure 6: Evolution of the accumulated time-averaged velocity components, velocity fluctuations quantities and scalar profiles for the selected mesh. Time-averaging starts from t = 4000.

observed the others studied variables (u, v, k, $u'v'$ and Q) and it was possible to draw the same conclusions. Therefore, considering the iLES methodology, we selected Mesh 3 for further analyses and studies.

To further guarantee that the selected time for convergence is enough, Fig. 6 shows the time-averaged values for u, v, k, $u'v'$ and Q. It is possible to observe that the u velocity profile reaches a converged profile very fast as this velocity dominates the flows and has small relative fluctuations. It's curious, tough, that the u velocity profile converges fast, but not the momentum thickness (see Fig. 5) as it only depends on that velocity profile (see Eq. 6). On the other hand, the v velocity profile takes much more time to reach a converged state, being it and the momentum thickness the ones responsible for the time selected for convergence. These previous results were also found by others studies in the literature (Brown and Roshko, 1974; Tenaud *et al.*, 2005). The fluctuation kinetic energy and the Reynolds stress component follow a similar behavior of each main component, i.e. u for k and v for $u'v'$, agreeing also with Tenaud *et al.* (2005). The scalar profile is shown in Fig. 6e and it also shows a fast convergence rate when compared to the v velocity profile, besides having a similar shape to the scalar profile of McMullan *et al.* (2007).

With the previous results, a statistically converged state of the flow was obtained with 36 FTCs after the transient had already left the domain. Therefore, the physics of the here studied mixing layer can be further explored and 3D simulations can start with the present set up.

4. CONCLUSIONS

The present study simulated a 2D mixing layer with a high-order method (Continuous Galerkin) in order to evaluate how much of the flow physics was captured at different levels of mesh refinement. Also, this research intended to study the transient flow due to the boundary and initial conditions and the statistically convergence of a 2D mixing layer in order to establish a reference for future mixing layer simulations and for future 3D simulations that the authors are going to perform. In this way, one can define a 2D mesh with the procedure herein performed and then extrude it to obtain a 3D mesh. Our future study will address the effects of local Re numbers along the mixing layer, 3D effects and differences to 2D simulations and a deeper analysis regarding the mixing process.

The CG method adopted a polynomial basis of order 3, thus resulting into a fourth order of spatial discretization. The mixing layer is defined by a velocity difference and a convective velocity of 1, a initial momentum thickess of 1 and a Re equal to 1000. The transient analysis showed that a time of 4 FTCs (flow-through cycles) or 4000 non-dimensional times were necessary to the transient effects had completely disappeared from the simulation. Also, a mesh study was performed in order to observe differences in the solution and guarantee that the mesh adopted was not too coarse, having in mind the iLES (uDNS) approach. Besides the transient, a convergence analysis was carried out and defined that 36 FTCs or 36000 non-dimensional times were necessary until the flow reached a statistically converged state, mainly because of the v velocity component and its fluctuations. The resolved scalar field behaved somehow similar to the main flow velocity component (u) when regarding the convergence rate, which results are confirmed by the literature. Ergo, the present study was successfully in simulating a 2D mixing layer with a high-order method.

5. ACKNOWLEDGEMENTS

The authors acknowledge support from CAPES (*Coordenação de Aperfeiçoamento de Pessoal de Nível Superior - Brasil* - Finance Code 001) and CNPq (*Conselho Nacional de Desenvolvimento Científico e Tecnológico - Brasil*), specially DGR who is a CNPq scholarship holder (Process number 141515/2021-0). RCM and VM acknowledge support from São Paulo Research Foundation (FAPESP) via grant 2020/10910-8. Also, the authors are thankful to all members of the LASCA laboratory group (ITA).

6. REFERENCES

Attili, A. and Bisetti, F., 2012. "Statistics and scaling of turbulence in a spatially developing mixing layer at Re = 250". *Physics of Fluids*, Vol. 24, No. 3, p. 035109. doi:10.1063/1.3696302.

Brown, G.L. and Roshko, A., 1974. "On density effects and large structure in turbulent mixing layers". *Journal of Fluid Mechanics*, Vol. 64, No. 4, p. 775–816. doi:10.1017/S002211207400190X.

Cantwell, C., Moxey, D., Comerford, A., Bolis, A., Rocco, G., Mengaldo, G., De Grazia, D., Yakovlev, S., Lombard, J.E., Ekelschot, D., Jordi, B., Xu, H., Mohamied, Y., Eskilsson, C., Nelson, B., Vos, P., Biotto, C., Kirby, R. and Sherwin, S., 2015. "Nektar++: An open-source spectral/hp element framework". *Computer Physics Communications*, Vol. 192, pp. 205–219. ISSN 0010-4655. doi:https://doi.org/10.1016/j.cpc.2015.02.008.

Clemens, N.T. and Mungal, M.G., 1992. "Two- and three-dimensional effects in the supersonic mixing layer". *AIAA Journal*, Vol. 30, No. 4, pp. 973–981. doi:10.2514/3.11016.

Ferreira, P.H., de Araújo, T.B., Carvalho, E.O., Fernandes, L.D. and Moura, R.C., 2022. "Numerical investigation of flow past bio-inspired wavy leading-edge cylinders". *Energies*, Vol. 15, No. 23. doi:10.3390/en15238993.

Foysi, H. and Sarkar, S., 2010. "The compressible mixing layer: an LES study". *Theoretical and Computational Fluid*

Dynamics, Vol. 24, pp. 565–588.

Gaster, M., Kit, E. and Wygnanski, I., 1985. "Large-scale structures in a forced turbulent mixing layer". *Journal of Fluid Mechanics*, Vol. 150, p. 23–39. doi:10.1017/S0022112085000027.

Kartha, A., Subbareddy, P.K. and Candler, G.V., 2020. "LES of subsonic reacting mixing layers". *Flow, Turbulence and Combustion*, Vol. 104, pp. 947–976.

Koochesfahani, M.M. and Dimotakis, P.E., 1986. "Mixing and chemical reactions in a turbulent liquid mixing layer". *Journal of Fluid Mechanics*, Vol. 170, p. 83–112. doi:10.1017/S0022112086000812.

Maghrebi, M.J. and Zarghami, A., 2010. "DNS of forced mixing layer." *International Journal of Numerical Analysis & Modeling*, Vol. 7, No. 1.

Martha, C.S., Blaisdell, G.A. and Lyrintzis, A.S., 2013. "Large eddy simulations of 2-D and 3-D spatially developing mixing layers". *Aerospace Science and Technology*, Vol. 31, No. 1, pp. 59–72. ISSN 1270-9638. doi: https://doi.org/10.1016/j.ast.2013.09.007.

Martins, Y. W. G.; Malatesta, V.M.R.C., 2021. "Numerical study of the flow past an inclined flat plate via spectral/hp element methods with novel stabilization". In *26th ABCM International Congress of Mechanical Engineering*. doi: https://doi.org/10.26678/ABCM.COBEM2021.COB2021-0750.

McMullan, W.A., Gao, S. and Coats, C.M., 2007. "A comparative study of inflow conditions for two- and three-dimensional spatially developing mixing layers using large eddy simulation". *International Journal for Numerical Methods in Fluids*, Vol. 55, No. 6, pp. 589–610. doi:https://doi.org/10.1002/fld.1482.

McMurtry, P.A., Jou, W.H., Riley, J. and Metcalfe, R.W., 1986. "Direct numerical simulations of a reacting mixing layer with chemical heat release". *AIAA Journal*, Vol. 24, No. 6, pp. 962–970. doi:10.2514/3.9371.

Mengaldo, G., Moxey, D., Turner, M., Moura, R.C., Jassim, A., Taylor, M., Peiró, J. and Sherwin, S., 2021. "Industry-relevant implicit large-eddy simulation of a high-performance road car via spectral/hp element methods". *SIAM Review*, Vol. 63, No. 4, pp. 723–755. doi:10.1137/20M1345359.

Miller, R.S., Madnia, C.K. and Givi, P., 1994. "Structure of a turbulent reacting mixing layer". *Combustion Science and Technology*, Vol. 99, No. 1-3, pp. 1–36. doi:10.1080/00102209408935423.

Moura, R., Mengaldo, G., Peiró, J. and Sherwin, S., 2017. "On the eddy-resolving capability of high-order discontinuous galerkin approaches to implicit LES / under-resolved DNS of euler turbulence". *Journal of Computational Physics*, Vol. 330, pp. 615–623. ISSN 0021-9991. doi:https://doi.org/10.1016/j.jcp.2016.10.056.

Moura, R., Peiró, J. and Sherwin, S., 2019. "Under-resolved DNS of non-trivial turbulent boundary layers via spectral/hp CG schemes". In *ERCOFTAC Workshop Direct and Large Eddy Simulation*. Springer, pp. 389–395. doi: https://doi.org/10.1007/978-3-030-42822-851.

Moura, R.C., Aman, M., Peiró, J. and Sherwin, S.J., 2020. "Spatial eigenanalysis of spectral/hp continuous galerkin schemes and their stabilisation via DG-mimicking spectral vanishing viscosity for high reynolds number flows". *Journal of Computational Physics*, Vol. 406, p. 109112. ISSN 0021-9991. doi:https://doi.org/10.1016/j.jcp.2019.109112.

Moura, R.C., Cassinelli, A., da Silva, A.F., Burman, E. and Sherwin, S.J., 2022. "Gradient jump penalty stabilisation of spectral/hp element discretisation for under-resolved turbulence simulations". *Computer Methods in Applied Mechanics and Engineering*, Vol. 388, p. 114200. ISSN 0045-7825. doi:https://doi.org/10.1016/j.cma.2021.114200.

Moxey, D., Cantwell, C.D., Bao, Y., Cassinelli, A., Castiglioni, G., Chun, S., Juda, E., Kazemi, E., Lackhove, K., Marcon, J., Mengaldo, G., Serson, D., Turner, M., Xu, H., Peiró, J., Kirby, R.M. and Sherwin, S.J., 2020. "Nektar++: Enhancing the capability and application of high-fidelity spectral/hp element methods". *Computer Physics Communications*, Vol. 249, p. 107110. ISSN 0010-4655. doi:https://doi.org/10.1016/j.cpc.2019.107110. URL `https://www.sciencedirect.com/science/article/pii/S0010465519304175`.

Papamoschou, D. and Roshko, A., 1988. "The compressible turbulent shear layer: an experimental study". *Journal of Fluid Mechanics*, Vol. 197, p. 453–477. doi:10.1017/S0022112088003325.

Pope, S.B., 2000. *Turbulent Flows*. Cambridge University Press. doi:10.1017/CBO9780511840531.

Stanley, S. and Sarkar, S., 1997. "Simulations of spatially developing two-dimensional shear layers and jets". *Theoretical and computational fluid dynamics*, Vol. 9, pp. 121–147.

Tenaud, C., Pellerin, S., Dulieu, A. and Ta Phuoc, L., 2005. "Large eddy simulations of a spatially developing incompressible 3D mixing layer using the v–ω formulation". *Computers Fluids*, Vol. 34, No. 1, pp. 67–96. ISSN 0045-7930. doi:https://doi.org/10.1016/j.compfluid.2004.03.003.

Yang, W., Zhang, H., Chan, C. and Lin, W., 2004. "Large eddy simulation of mixing layer". *Journal of Computational and Applied Mathematics*, Vol. 163, No. 1, pp. 311–318. doi:https://doi.org/10.1016/j.cam.2003.08.076. Proceedings of the International Symposium on Computational Mathematics and Applications.

Zhang, C.X., Liu, Y., Fu, B.S. and Yu, X.J., 2018. "Direct numerical simulation of subsonic–supersonic mixing layer". *Acta Astronautica*, Vol. 153, pp. 50–59. ISSN 0094-5765. doi:https://doi.org/10.1016/j.actaastro.2018.10.004.

7. RESPONSIBILITY NOTICE

The authors are solely responsible for the printed material included in this paper.